

# Mechanical properties of tungsten alloys with $Y_2O_3$ and titanium additions

M.V. Aguirre<sup>a,\*</sup>, A. Martín<sup>b</sup>, J.Y. Pastor<sup>b</sup>, J. Llorca<sup>b,c</sup>, M.A. Monge<sup>d</sup>, R. Pareja<sup>d</sup>

<sup>a</sup>Departamento de Tecnologías Especiales Aplicadas a la Aeronáutica, Universidad Politécnica de Madrid, E.U.I.T. Aeronáutica, 28040 Madrid, Spain

<sup>b</sup>Departamento de Ciencia de Materiales-CISEM, Universidad Politécnica de Madrid.E.T.S. Ingenieros de Caminos, 28040 Madrid, Spain

<sup>c</sup>Instituto Madrileño de Estudios Avanzados en Materiales (Instituto IMDEA-Materiales), Ingenieros de Caminos, 28040 Madrid, Spain

<sup>d</sup>Departamento de Física, Universidad Carlos III de Madrid, 28911 Leganés, Spain

## A B S T R A C T

In this research the mechanical behaviour of pure tungsten (W) and its alloys (2 wt.% Ti–0.47 wt.%  $Y_2O_3$  and 4 wt.% Ti–0.5 wt.%  $Y_2O_3$ ) is compared. These tungsten alloys, have been obtained by powder metallurgy. The yield strength, fracture toughness and elastic modulus have been studied in the temperature interval of 25 °C to 1000 °C. The results have shown that the addition of Ti substantially improves the bending strength and toughness of W, but it also dramatically increases the DBTT. On the other hand, the addition of 0.5%  $Y_2O_3$ , is enough to improve noticeably the oxidation behaviour at the higher temperatures. The grain size, fractography and microstructure are studied in these materials. Titanium is a good grain growth inhibitor and effective precursor of liquid phase in HIP. The simultaneous presence of  $Y_2O_3$  and Ti permits to obtain materials with low pores presence.

## 1. Introduction

W is one of the candidate materials for manufacturing of plasma facing components in future fusion power reactors because of its good characteristics as a refractory material, which include sputtering resistance, thermal shock resistance and low tritium retention [1]. Nevertheless, good mechanical properties at high temperature are required for these materials.

On the other hand, tungsten improves substantially its mechanical strength and toughness at high temperature through solid solution or particles dispersion, such as titanium or yttrium oxide, respectively [2]. One of the limitations of tungsten alloys for plasma facing components is the high ductile-to-brittle transition temperature (DBTT), which is normally above room temperature [3]. The DBTT of tungsten alloys depends on mechanical and microstructural factors, thus, the addition of different elements or particles modifies this temperature value. The sintering process is the adequate method to obtain solid solutions and particle dispersions if the recrystallization temperature is high enough and the growth grain can be inhibited during the sintering.

The main purpose of the present investigation is to study the mechanical behavior in the temperature interval from 25 °C to 1000 °C and the mechanism involved in the fracture of two tungsten alloys, obtained by hot isostatic pressure. To achieve

this, three-point bending and fracture toughness tests are performed.

## 2. Experimental

### 2.1. Materials

Two tungsten alloys containing 2 wt.% Ti–0.47 wt.%  $Y_2O_3$  and 4 wt.% Ti–0.5 wt.%  $Y_2O_3$  have been studied. Both of them were obtained by hot isostatic pressure of blended or ball milled powders. The starting materials were different powders: tungsten (99.9% purity and 14  $\mu\text{m}$  of average grain size), titanium (99.8% purity and particle size of 20  $\mu\text{m}$ ) and nanoparticles of  $Y_2O_3$  (99.5% purity and diameter in the range 10–50 nm). The manufacturing process was developed under Ar atmosphere. The sintering was carried out by hot isostatic pressure in two stages: the first at 1277 °C and 195 MPa of pressure, and the second at 1700 °C and the same pressure [4].

These alloys were supplied in a billet with nominal dimensions of 30 mm diameter and 50 mm length. Prismatic samples with  $2 \times 2 \times 25 \text{ mm}^3$  were prepared by electro-discharge machining. A notch of 400  $\mu\text{m}$  in depth and tip radius of approximately 150  $\mu\text{m}$  was introduced with a diamond saw in the samples for fracture toughness tests.

Three materials are used as reference materials, pure tungsten and two tungsten alloys with 4 wt.% Ti and 0.5 wt.%  $Y_2O_3$ , respectively. The mechanical behavior with temperature, the microstructural analysis and the effect of titanium and yttrium oxide additions in these simple alloys have previously been studied [2].

## 2.2. Experimental methods

The elastic modulus at room temperature,  $E_0$ , was measured on prismatic samples using the impulse excitation technique. Cycles of load charge and discharge (each 200 °C) were performed in three-point bending test keeping the material in the lineal elastic region and well below its maximum strength. The evolution of the elastic modulus with temperature was studied by the slope change of the load and load-point displacement curve. The bending tests and the fracture toughness tests were performed under stroke control at 100  $\mu\text{m}/\text{min}$ . The loading spans were 16 and 12 mm for bending and fracture toughness tests, respectively. The yield stress was computed by Bernoulli equations for flexural beam with 0.2% of deformation. The  $K_Q$  was calculated by the general expression of stress intensity factor [5]. All the mechanical tests were performed under ambient atmosphere.

The fracture surfaces of *post-mortem* samples were studied by scanning electron microscope. The presence of oxidation products impeded the observation of the fracture surfaces in samples tested at high temperature. Then these broken samples were mounted in epoxy resin and prepared by polishing and etching (Murakami and Kroll reagents) to analyze the cross section. The mounted samples were studied in the scanning electron microscope equipped with energy dispersive X-ray microanalysis to ascertain the deformation and failure micromechanism involved in the fracture process as well as the present phases.

## 3. Results and discussion

### 3.1. Mechanical properties

The *elastic modulus* at room temperature,  $E_0$ , is similar to that of the reference materials although the value of the W–2% Ti–0.47%  $\text{Y}_2\text{O}_3$  alloy is somewhat lower. In these alloys this evolution does not drop as strongly as in pure W and W–4%Ti [2]. Even the W–4% Ti–0.5%  $\text{Y}_2\text{O}_3$  material shows a behavior similar to that of W–0.5%  $\text{Y}_2\text{O}_3$ . Thus, this confirms that the presence of the yttrium oxide improves the oxidation resistance and consequently the alloys enhance their mechanical properties at high temperature. It should be note that the tests were carried out in oxidating atmosphere, thus, the decreasing in the elastic modulus is due to loss of material because of the oxidation process. The  $\sigma$ – $\varepsilon$  curves correspond to a linear elastic behavior, even at the highest temperatures.

In Fig. 1 are drawn the *yield strengths* ( $\sigma_{0.2\%}$ ) for tests with plastic deformation and the flexural strength for tests with brittle behavior. The bending strength of W–2% Ti–0.47%  $\text{Y}_2\text{O}_3$  is almost constant with temperature and in spite of the starting values are low presents a high value at high temperature. By contrast, the W–4% Ti–0.5%  $\text{Y}_2\text{O}_3$  starts with a low value at room temperature but the increasing of the resistance is similar to that of W–4% Ti and reaches a higher value at 800 °C due to the effect of yttrium oxide. Above this temperature the instability of the titanium oxide causes a strongly drop in the curve.

The recorded values of load and displacement in the *fracture toughness* tests with SENB samples depend strongly on the dimensions of material. Thus, these results must be considered as reference values. It should be noted that some reference materials show macroscopic plastic deformation according to the test temperature increases. Therefore, the calculated values could be considered values of “apparent fracture toughness” (obtained by applying the value of the maximum load in the expressions of stress intensity factor) and they only give an idea of its evolution with temperature. Fig. 2 shows the evolution with temperature of this property, similar to the bending strength curve.

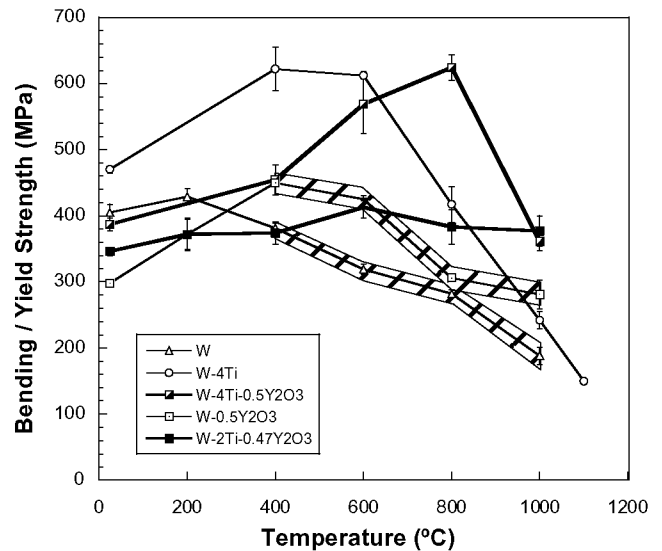


Fig. 1. Bending or yield strength of the samples tested in three-point bending. Shaded values stand for the yield strength at 0.2% of plastic strain (material with plastic deformation before fracture). Non shaded values stand for bending strength (tests with a linear response until fracture).

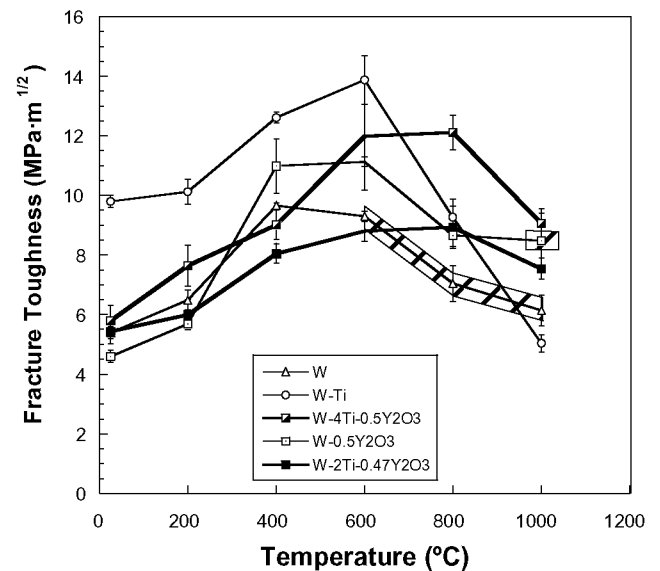


Fig. 2. Evolution of fracture toughness with test temperature. Shaded values stand for “apparent fracture toughness” (tests with substantial plastic deformation before maximum load).

The fracture toughness of these alloys is low because of the tests were carried out in oxidizing atmosphere. Despite this, the values do not have a trend to decrease as fast as those of W–4% Ti and the values obtained at 1000 °C are similar to those of W–0.5%  $\text{Y}_2\text{O}_3$ . This again proves that the presence of  $\text{Y}_2\text{O}_3$  improves the oxidation behavior at high temperature and consequently a better mechanical behavior is obtained. However the low values of toughness at room temperature indicate that the presence of titanium can not improve this property because of pores produce a crack effect. It should be taken into account that these values could overestimate the actual toughness of the materials because the notch was not a true crack.

### 3.2. Fractography

According to the curves of the bending test and fracture toughness, the specimens show a brittle fracture at any temperature in both materials. The samples present a flat fracture surface perpendicular to the tensile stress with a crystalline aspect. Both materials show similar fracture characteristics: brittle intergranular fracture due to the discohension among tungsten particles and cleavage or discohension of lattice planes. These are typical patterns in BCC metals below the DBTT [6]. These characteristics are presented up 400 °C, but above this temperature only some specimens without oxidation products could be observed. The cleavage is scarcely present at this temperature, in smaller numbers in W-2% Ti-0.47% Y<sub>2</sub>O<sub>3</sub> alloy. The cleavage character is associated with DBTT, so the titanium content increases this temperature in tungsten even with contents of 2 wt.%.

The presence of many and small pores has been observed mainly on the grain boundaries and penetrating to some depth in the particles of tungsten (Fig. 3). This porosity is less abundant in W-4% Ti-0.5% Y<sub>2</sub>O<sub>3</sub> material and is not present in the reference material W-4% Ti. Thus, the presence of titanium and Y<sub>2</sub>O<sub>3</sub> simultaneously could catalyze a reaction with generating of gaseous products during sintering process what causes the appearance of porosity.

The analysis of the cross section behind the fracture surface reveals the morphology of the grains under the surface. The surface profile is nearly a polygonal line corresponding to the intergranular fracture and cleavage (Fig. 4). In all of the samples grain deformation, sliding of boundary grain and voids growth do not have been observed up to 600 °C. Beyond this temperature, the grains of the fracture surface have disappeared forming a layer of oxidation products.

### 3.3. Microstructure

Both of these alloys primarily show two types of phases: lagoons of titanium and tungsten grains. A solid solution Ti-W has been formed because of titanium diffusion along the grain boundaries of tungsten during sintering. However, tungsten atoms diffusion has not been observed in titanium pools. The cross section of fracture surface reveals the morphology of these phases. Tungsten alloy with 2% Ti-0.47% Y<sub>2</sub>O<sub>3</sub> presents Ti lagoons and tungsten particles of different sizes. The large lagoons tend to be more elon-

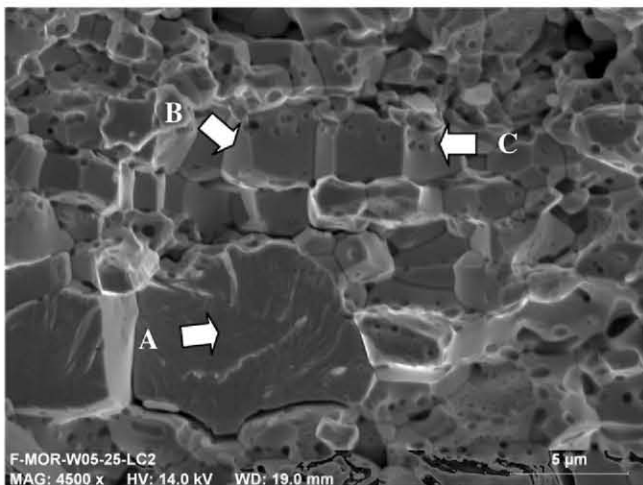


Fig. 3. SEM micrograph showing the fracture surface with intergranular porosity of W-2% Ti-0.47% Y<sub>2</sub>O<sub>3</sub> alloy (bending tested at 25 °C). Cleavage (A), aligned W grains (B) and porosity below the boundary grain (C).

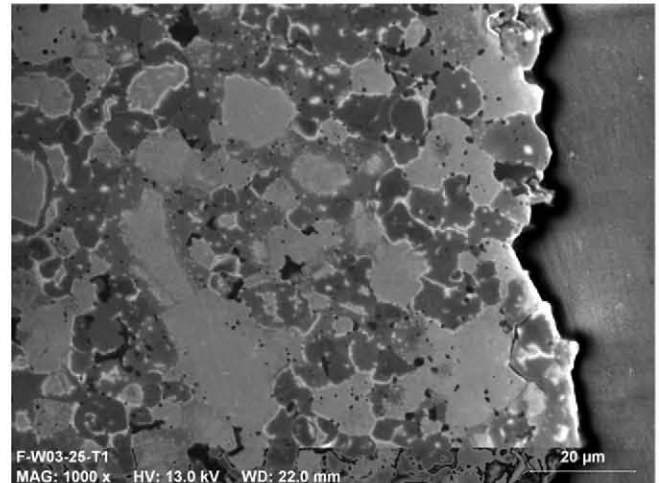


Fig. 4. Cross section showing the fracture surface profile in W-4% Ti-0.5% Y<sub>2</sub>O<sub>3</sub> alloy (bending tested at 25 °C). Sample etched with Murakami reagent.

gated than those in W-4% Ti-0.5% Y<sub>2</sub>O<sub>3</sub>. Some of tungsten particles have an elongated or fragmented shape as aligned grains quite parallel to titanium pools. In addition, a dark zone around these lagoons can be distinguished according to the solid solution formed due to titanium diffusion in tungsten grains (Fig. 5). On the other hand the distribution of Ti pools on the W-4% Ti-0.5% Y<sub>2</sub>O<sub>3</sub> seems equal to that seen in W-4% Ti. The aligned tungsten grains do not have been observed in this alloy. In both materials the solid solution formed around the W particles is thicker than the one observed in W-4% Ti. Therefore, the presence of Y<sub>2</sub>O<sub>3</sub> favors titanium diffusion to form larger zones of solid solution.

A rich yttrium phase was detected in the interface between titanium pools and tungsten grains. Phase-shaped bones (corresponding to phases melt during sintering process) observed in W-0.5% Y<sub>2</sub>O<sub>3</sub> have not been detected in these alloys. This means that the presence of titanium hinders tungsten diffusion in Y<sub>2</sub>O<sub>3</sub> avoiding the formation of low melting point phases.

The samples were etched with hydrogen peroxide to reveal the boundary grain. The presence of a solid solution surrounding the tungsten particles impeded to obtain micrographs with good contrast. The estimation of grain size could be made by comparison with the reference materials micrographs. The alloys have a similar grain size and size distribution to those of the W-4% Ti material (Fig. 6) with less deviation [2]. The maximum and minimum grain sizes

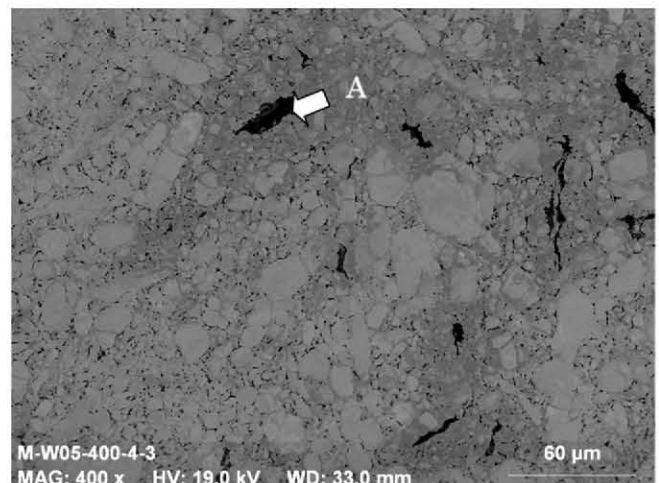
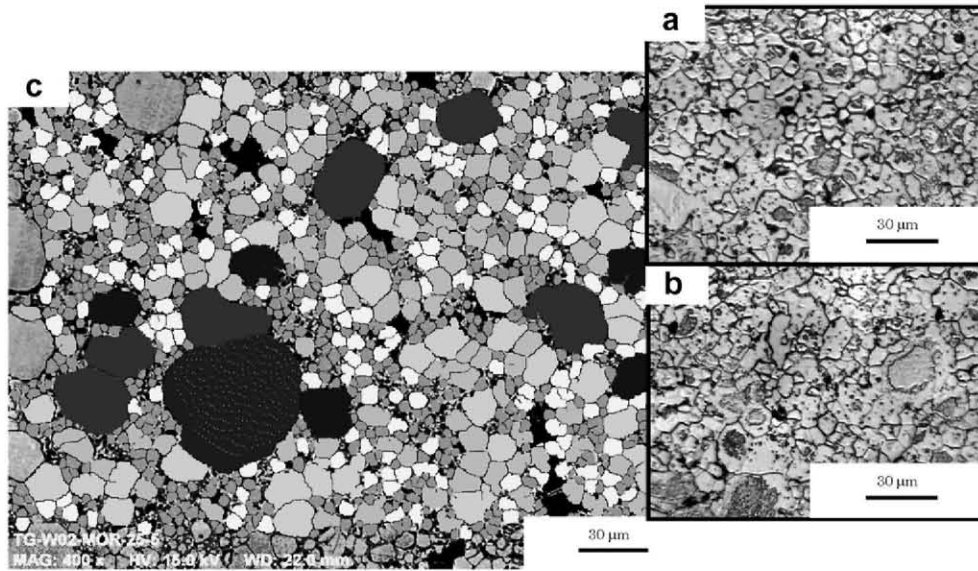


Fig. 5. Micrograph of W-2% Ti-0.47% Y<sub>2</sub>O<sub>3</sub> alloy bending tested at 400 °C (etched with Murakami reagent). (A) Ti pools.



**Fig. 6.** Micrographs for grain size estimation. (a and b) W-4% Ti-0.5% Y<sub>2</sub>O<sub>3</sub> and (c) W-4% Ti (reference material).

are less different allowing a more homogeneous distribution. The average grain size is slightly larger in these alloys than in W-4% Ti.

#### 4. Conclusions

The addition of titanium favors the densification of tungsten in sintering. In addition, titanium inhibits the grain growth in tungsten and reduces its diffusion on Y<sub>2</sub>O<sub>3</sub> particles avoiding their decomposition. Titanium has a negative effect on DBTT, raising this temperature in tungsten at least 600 °C. Titanium improves the mechanical behavior of tungsten with temperature, but makes it more brittle.

The presence of Y<sub>2</sub>O<sub>3</sub> at about 0.5 wt.% increases the oxidation resistance of tungsten consequently improving the mechanical behavior at high temperature. The yttrium oxide enhances titanium diffusion on tungsten favoring the formation of Ti-W solid solution. Y<sub>2</sub>O<sub>3</sub> seems does not have influence on DBTT.

The simultaneous presence of Ti and Y<sub>2</sub>O<sub>3</sub> involves the addition of side effects but could reduces the densification effect of titanium.

#### Acknowledgements

This investigation was supported by the EURATOM/CIEMAT association through contract TW6-TTMA-002-EFDA, by the Comunidad de Madrid (programs S-S2009/MAT-1585 and S2009/ENE-1679) and by the Spanish Ministry of Science and Innovation (CSD00C-06-14102 and MAT 2009-13979-C03-02).

#### References

- [1] J.W. Davis, V.R. Barabash, A. Makhankov, L. Plöchl, K.T. Slattery, *J. Nucl. Mater.* 258–263 (1998) 308–312.
- [2] M.V. Aguirre, A. Martin, J.Y. Pastor, J. Llorca, M.A. Monge, R. Pareja, *Metall. and Mat. Trans. A* 40 (2009) 2283–2290.
- [3] P. Gumbsch, J. Riedle, A. Hartmaier, H.F. Fischmeister, *Science* 282 (1998) 1293–1295.
- [4] M.A. Monge, M.A. Auger, T. Leguey, Y. Ortega, L. Bolzoni, E. Gordo, R. Pareja, *J. Nucl. Mater.* 386–388 (2009) 317–613.
- [5] G. Guinea, J.Y. Pastor, J. Planas, M. Elices, *Int. J. Fracture* 89 (1998) 103–116.
- [6] M. Faleschini, H. Kreuzer, D. Kiener, R. Pippan, *J. Nucl. Mater.* 367–370 (2007) 800–805.